Title
High-Precision Control of Plasma Drug Levels Using Feedback-Controlled Dosing

Journal
ACS Pharmacology & Translational Science, 1(2)

ISSN
2575-9108

Authors
Arroyo-Currás, Netzahualcóyotl
Ortega, Gabriel
Copp, David A
et al.

Publication Date
2018-11-09

DOI
10.1021/acsptsci.8b00033

ACS Pharmacology & Translational Science

Article

Cite This: ACS Pharmacol. Transl. Sci. 2018, 1, 110−118

pubs.acs.org/ptsci

High-Precision Control of Plasma Drug Levels Using Feedback-Controlled Dosing

Netzahualcóyotl Arroyo-Currás,[*,†] Gabriel Ortega,[‡,§,∥] David A. Copp,[⊥] Kyle L. Ploense,[‡,#] Zoe A. Plaxco,[‡,§] Tod E. Kippin,[#,▽] João P. Hespanha,[⊥] and Kevin W. Plaxco[*,‡,§]

[†]Department of Pharmacology and Molecular Sciences, Johns Hopkins School of Medicine, Baltimore, Maryland 21205, United States

[‡]Department of Chemistry and Biochemistry, [§]Center for Bioengineering, [⊥]Center for Control, Dynamical Systems, and Computation, [#]Department of Psychological and Brain Sciences, and [▽]The Neuroscience Research Institute and Department of Molecular, Cellular, and Developmental Biology, University of California Santa Barbara, Santa Barbara, California 93106, United States

[∥]CIC bioGUNE, Bizkaia Technology Park, Ed. 801A, 48160, Derio, Spain

Supporting Information

ABSTRACT: By, in effect, rendering pharmacokinetics an experimentally adjustable parameter, the ability to perform feedback-controlled dosing informed by high-frequency in vivo drug measurements would prove a powerful tool for both pharmacological research and clinical practice. Efforts to this end, however, have historically been thwarted by an inability to measure in vivo drug levels in real time and with sufficient convenience and temporal resolution. In response, we describe a closed-loop, feedback-controlled delivery system that uses drug level measurements provided by an in vivo electrochemical aptamer-based (E-AB) sensor to adjust dosing rates every 7 s. The resulting system supports the maintenance of either constant or predefined time-varying plasma drug concentration profiles in live rats over many hours. For researchers, the resultant high-precision control over drug plasma concentrations provides an unprecedented opportunity to (1) map the relationships between pharmacokinetics and clinical outcomes, (2) eliminate inter- and intrasubject metabolic variation as a confounding experimental variable, (3) accurately simulate human pharmacokinetics in animal models, and (4) measure minute-to-minute changes in a drug's pharmacokinetic behavior in response to changing health status, diet, drug−drug interactions, or other intrinsic and external factors. In the clinic, feedback-controlled drug delivery would improve our ability to accurately maintain therapeutic drug levels in the face of large, often unpredictable intra- and interpatient metabolic variation. This, in turn, would improve the efficacy and safety of therapeutic intervention, particularly for the most gravely ill patients, for whom metabolic variability is highest and the margin for therapeutic error is smallest.

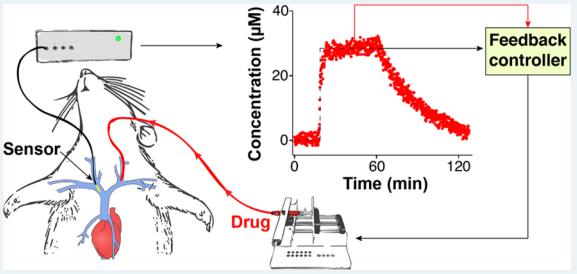

KEYWORDS: *aminoglycosides, antibiotics, therapeutic drug monitoring, controlled drug delivery, biosensing*

INTRODUCTION

A technology supporting feedback-controlled drug delivery informed by high-frequency in vivo drug measurements would find important applications in both pharmacological research and in clinical practice. Such a technology would, for example, allow researchers to treat pharmacokinetic variability as an experimentally controllable parameter, enabling studies of the reproducibility of therapeutic outcomes when such variability is effectively eliminated (e.g., to make all animals in a test cohort exhibit the same maximum drug concentration and the same area under the curve). It would likewise enable the accurate simulation of human pharmacokinetics in animal models, rendering them better mimics of human physiology.[1−4] Ultimately, such a technology could similarly prove of value in the clinic, where it could be used to optimize moment-to-moment dosing in response to a patient's changing metabolism, ensuring that a therapy's benefits are maximized while its risks are minimized.[5−9]

The potential scientific and clinical impact of feedback-controlled drug delivery has long been recognized.[5,6,8,10] Its realization, however, has historically been thwarted by an inability to measure in vivo drug levels in real time and with sufficient convenience and temporal resolution. That is, while established technologies exist for the real-time measurement of a handful of neurotransmitters (the monoamines,[11−16] glutamate,[17,18] adenosine,[19] and acetylcholine[18,20,21]) and metabolites (e.g., glucose,[18,22−25] lactate,[18,26] and oxygen[18,25,27]) in the living body, each of these is reliant on the specific chemical reactivity of the target (e.g., the direct

Received: August 29, 2018
Published: October 5, 2018

DOI: 10.1021/acsptsci.8b00033
ACS Pharmacol. Transl. Sci. 2018, 1, 110−118

electrochemical oxidation of monoamines or the enzymatic oxidation of glucose) and thus is not generalizable to the detection of other molecules. Recently, however, we have developed in vivo electrochemical aptamer-based (E-AB) sensors, the first ever in vivo sensing platform that is both (1) able to provide convenient, real-time, seconds-resolved molecular measurements in the living body[28] and (2) independent of the chemical reactivity of its target, and thus able to detect specific drugs.[29,30] Exploiting this we have achieved here the first ever example of feedback-controlled drug delivery informed by high-frequency in vivo drug concentration measurements. By actively adjusting dosing every seven seconds, the resultant control not only achieves the high-precision (±10%) maintenance of constant drug concentrations (over many hours), but can also generate predefined, time-varying concentration profiles that include the ability to simulate near-identical pharmacokinetics from animal to animal (equivalent to eliminating pharmacokinetic variation) and the accurate simulation of human pharmacokinetics in a rat model.

RESULTS AND DISCUSSION

E-AB sensors comprise a redox-reporter-modified aptamer that is attached to an interrogating electrode (Figure 1A). Upon target binding the efficiency of electron transfer from the reporter to the electrode is altered,[29,33,34] presumably due to a binding-induced conformational change. This, in turn, produces an easily measurable change in current when the sensor is interrogated electrochemically using square-wave voltammetry.[35−37] Because this signaling mechanism is independent of the chemical reactivity of the target, E-AB sensors can be and have been developed against a wide variety of targets.[31,35,38−48] Their signaling mechanism also renders E-AB sensors reagentless, reversible, and selective enough to support measurements in situ in the living body,[28,32,37,49] attributes critical to the task of performing continuous, in vivo measurements. Building on these advantages,[28,32,37,42,49] here we have adapted indwelling E-AB sensors to the problem of achieving high-precision, feedback-controlled drug delivery (Figure 1). Specifically, from among the large set of E-AB sensors developed to date[31,35,38−48] we selected an aminoglycoside sensor[28,40,42] as the test bed with which to demonstrate such delivery, as the therapeutic windows of these important, last-line-of-defense antibiotics are narrow, greatly complicating their proper dosing.[50] From among the aminoglycosides that this sensor is capable of measuring we selected tobramycin as our target because of the crucial importance of actively managing its plasma levels to prevent irreversible drug-induced toxicity.[51,52]

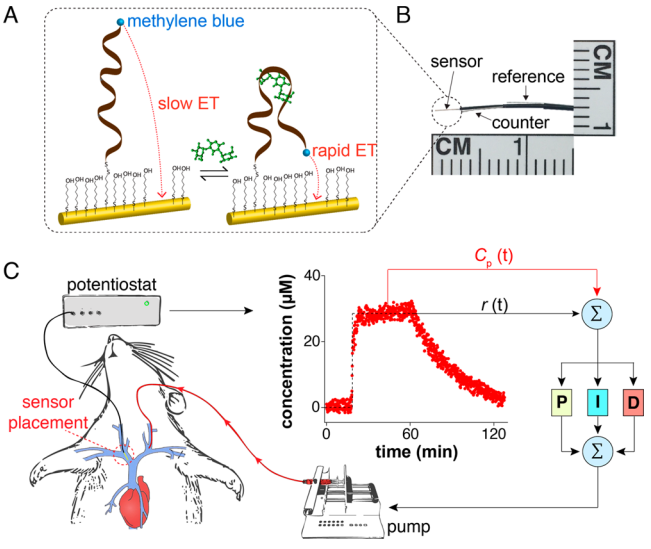

Figure 1. Closed-loop, feedback-controlled drug delivery. (A) E-AB sensors consist of an electrode-attached aptamer modified with a redox reporter (here methylene blue). Upon target binding the aptamer undergoes a conformational change that alters the rate of electron transfer from the reporter in a manner monotonically related to target concentration.[31] (B) With a diameter of ∼300 μm, E-AB sensors are small enough to deploy using a 22-gauge catheter; for the studies here we employed jugular placements.[32] (C) Using the real-time, seconds-resolved concentration information provided by such indwelling E-AB sensors as input to a feedback control algorithm we have here demonstrated the ability to actively adjust dosing rates every 7 s via an infusion pump delivering the drug into the opposite jugular. At each time point the controller computes the difference between the drug concentration reported by the sensor and a user-defined reference concentration and, based on proportional, integral, and derivative terms, calculates the precise drug dosing rate needed to best achieve the concentration desired at that moment.

To create the feedback control loop we first fabricated aminoglycoside-detecting E-AB sensors that are small enough[32] to emplace in situ inside the jugular vein of a live rat using a 22-gauge catheter (Figure 1B). We coupled the output of this sensor to a proportional-integral-derivative (PID) controller that computes an appropriate dosing rate based on the difference between the drug concentration this sensor measures, $C_p(t)$, and a user-defined fixed or time-varying reference concentration, $r(t)$ (Figure 1C). The PID controller comprises three terms: a term proportional to the difference between the observed and reference concentrations and weighted by the proportional gain, P; a term accounting for the integral of the difference between the observed and reference concentrations over time and weighted by the integral gain, I; and a term proportional to the derivative of the difference between the observed and reference concentrations and weighted by the derivative gain, D. Broadly, the proportional and integral terms adjust the instantaneous infusion rate to push the loop to achieve the desired concentration, while the "predictive" derivative term renders the loop stable with respect to system uncertainty; more details of PID control can be found in the literature.[53,54] To close the loop we used the output of this controller to adjust (every seven seconds) the rate with which a syringe pump delivers the drug via intravenous infusion (Figure 1C). Prior to attempting feedback-controlled drug delivery we adjusted the gains of all three terms in trial runs, first in vitro in flowing buffer (Figure S1) and then in situ in the veins of live rats (Figure S2).

E-AB guided feedback-control enables the high-precision maintenance of constant plasma drug concentrations in live animals. As a first demonstration of this we explored the system's ability to rapidly achieve and accurately hold plasma drug levels at three fixed concentrations. Specifically, for each of three animal subjects we measured a 20 min baseline before initiating a PID-controlled infusion aimed at achieving constant, predefined plasma levels of 80, 50, or 20 μM (Figure 2). Despite presumably large metabolic differences between the subjects (two males and one female varying in weight from 280 to 450 g) the feedback-controlled infusions achieved sustained drug levels within ±5 μM of the specified

DOI: 10.1021/acsptsci.8b00033
ACS Pharmacol. Transl. Sci. 2018, 1, 110−118

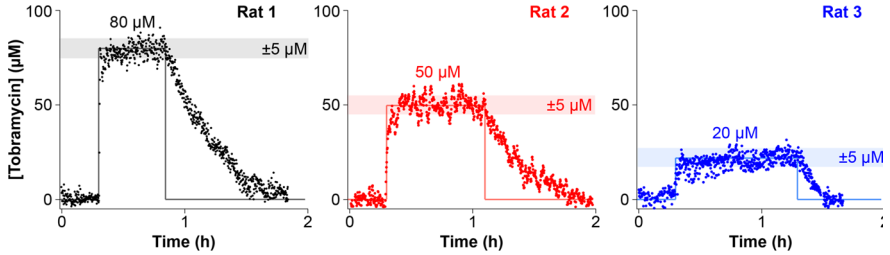

Figure 2. E-AB-driven feedback-controlled dosing supports unprecedentedly high-precision control over in vivo drug levels. Here, for example, we present feedback-controlled pharmacokinetic profiles in which the plasma tobramycin concentrations were held at set points of 80, 50, or 20 μM for 40, 50, and 60 min, respectively, in three different rats. The precision afforded by adjusting the dosing rate every 7 s using real-time concentration measurements is reflected in a variance of only a few micromolar around the desired concentration.

concentration set points in all three using the same set of PID gain parameters. This level of precision far exceeds that achieved by the constant-rate drug infusions that are currently state of the art for antibiotic dosing.[55,56] For example, when we perform constant-rate intravenous infusions of tobramycin (10 mg/kg) into two male rats (360 and 420 g) we observe far poorer precision in reaching and maintaining constant plasma drug concentrations (Figure S3).

Using E-AB-driven feedback control we can easily achieve the maintenance of constant plasma tobramycin concentrations centered within the drug's narrow therapeutic window. We demonstrated this by holding tobramycin at 10 times the drug's minimum inhibitory concentration, a value below that considered toxic in humans yet high enough to remain effective.[55,57] In this experiment we reached the desired concentration within 30 min of the onset of control and then actively held that concentration for 4 h (Figure 3A; Figure S4). Of note, the time frame of this control was limited by the maximum time we are allowed to keep animals under anesthesia (to avoid toxic exposure to the anesthetic isoflurane) and not by any failure of the sensor or the resulting feedback control.

The controller maintains constant plasma drug levels even in the face of significant metabolic variation (Figure 3A). Moreover, its ability to do so provides a means of determining the magnitude of this variation with unprecedented, minute-scale time resolution. Once plasma drug levels have reached the desired concentration, the drug's instantaneous elimination half-life, $t_{1/2}$ (in min), can be derived from the infusion rate, R (in μg·min^{-1}), via[58]

$$t_{1/2}(t) = \ln 2 \cdot \text{M.W.} \cdot V_D \cdot C_{P(t)}/R(t) \quad (1)$$

where M.W. is the molecular weight of the drug in daltons, C_P is the drug's plasma concentration in molar units, and V_D is the volume of distribution (in liters), which can be determined separately from the pharmacokinetic profiles of intravenous injections (Figure S5) and is assumed to be approximately constant throughout the experiment. The resultant plot of the drug's changing elimination half-life illustrates the significant (here ~3-fold) fluctuations seen for the metabolism (excretion) of this drug in rats over the course of just a few hours (Figure 3B), which presumably occurs due to increasing kidney clearance associated with the intravenous fluid delivered during dosing.[59,60]

While the ability to maintain plasma drug levels at a fixed value (e.g., centered within the therapeutic window) should be of significant clinical value,[61−65] achieving similarly precise control over defined, time-varying profiles is likely also of value. Such control, for example, could be used to reduce

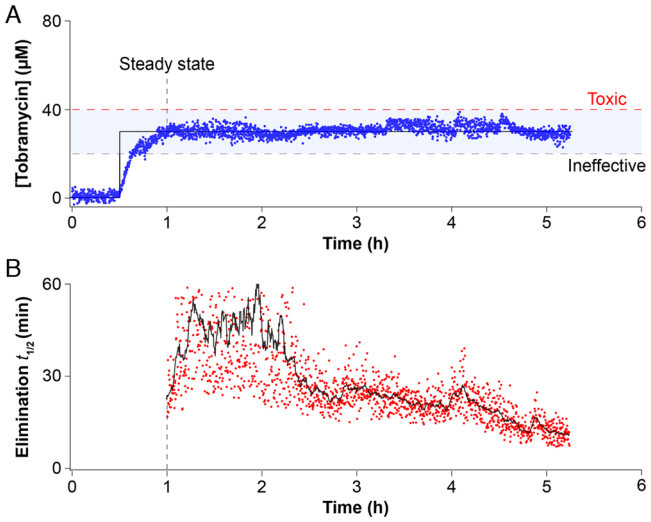

Figure 3. Feedback-controlled, multihour maintenance of therapeutic drug levels. PID-controlled drug infusions actively adjust dosing in response to metabolic fluctuations within a living subject. (A) Here, for example, we used feedback control to hold the plasma tobramycin level constant at a concentration 10-fold above the drug's MIC_{90} (the minimum inhibitory concentration for 90% of clinical isolates[57]) for approximately 4 h. (Longer runs are precluded due to animal welfare concerns that limit the time animals can be kept under anesthesia to avoid toxic exposure to the anesthetic gas isoflurane). (B) The elimination half-life of the drug, which can be determined from the instantaneous dosing rate required to maintain plasma concentrations at the desired concentration (eq 1), varies by more than a factor of 3 within this one subject over the course of this experiment, highlighting the need for improved drug delivery mechanisms. The black curve reflects a 3 min rolling average.

subject-to-subject pharmacokinetic variation, an experimental variable that often confounds drug discovery efforts.[66] To demonstrate our ability to precisely achieve such profiles we compared two groups of rats, one receiving manual, intramuscular (IM) injections of tobramycin at a dose scaled to their body surface area (an approach generally thought to correct for intersubject varability[67]) and the other receiving PID-controlled intravenous infusions following a predefined pharmacokinetic function mimicking the pharmacokinetic profile of a specific IM injection within a specific individual (Figure 4). As expected, the group receiving IM injections exhibited significant pharmacokinetic variability; that is, 30% standard deviation between areas under the three pharmacokinetic curves (Figure 4A). In contrast, the areas under the curve for the group receiving feedback-controlled infusions

DOI: 10.1021/acsptsci.8b00033
ACS Pharmacol. Transl. Sci. 2018, 1, 110−118

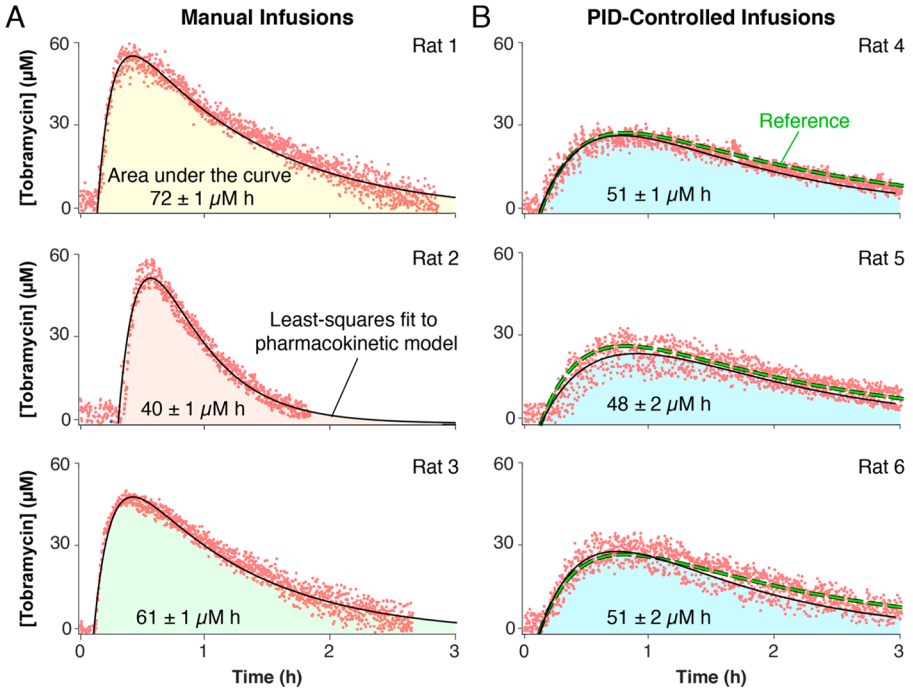

Figure 4. Eliminating subject-to-subject variability in drug exposure. Intersubject metabolic variability can confound studies of the relationships between pharmacokinetics and therapeutic outcomes. The high precision control over in vivo drug levels afforded by E-AB-driven feedback control provides a means of circumventing this confounding variability. (A) As shown, for example, the intramuscular administration of empirically determined doses of tobramycin (by calibrating them against body surface area)[68] results in significant (30% standard deviation) subject-to-subject variability in drug exposure as measured by the area under the curve. (B) In contrast, PID-controlled delivery following a programmed pharmacokinetic function (here we imposed a one compartment pharmacokinetic model with first order drug absorption and elimination kinetics) results in an order of magnitude improvement in the precision with which the area under the curve can be reproduced between animals (4% standard deviation).

exhibited only 4% standard deviation despite similarly varying in size and body surface area (Figure 4B).

To find the source of this improvement we performed regression analyses of our data using a one compartment pharmacokinetic model with first-order absorption and elimination kinetics[58] and then calculated the relative standard deviation between the pharmacokinetic parameters obtained from the relevant pharmacokinetic profiles. Doing this we determined that the improved precision we achieve originates from actively adjusting dosing in response to fluctuations of the rate of elimination (Figure 5); in other words, our controller is successfully responding to differences in the pharmacokinetics of different rats to ensure that the total area under the curve remains effectively identical between them.

A third potentially important research application of feedback-controlled drug delivery would be to emulate human drug exposure profiles in animal models. Such "humanization" of animal pharmacokinetics would allow us to determine the effects of human-like plasma drug-time profiles (rather than the typically much more rapid unconstrained pharmacokinetics of the animal) on diseases being studied in animal models, such as infection with human pathogens or the treatment of human xenograft tumors, and to better determine the most effective dose in the face of significant interspecies differences in drug pharmacokinetics.[1,2] Here, for example, we used this approach to generate a human-like pharmacokinetic profile for tobramycin in a rat. To do this we first extracted pharmacokinetic data corresponding to 10 human patients from the clinical literature[55] and performed regression analysis to obtain the average human profile. Using

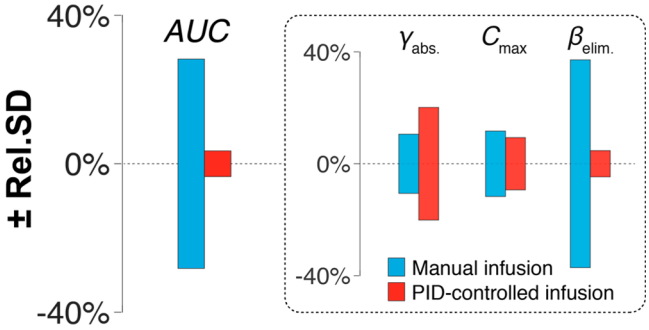

Figure 5. Feedback-controlled drug delivery greatly improves control over drug exposure. Here we present the relative standard deviation of four pharmacokinetic parameters determined by regression analysis of the profiles shown in Figure 4: the area under the curve (*AUC*), the rate of drug absorption ($\gamma_{abs.}$), the maximum plasma concentration (C_{max}), and the rate of elimination (β_{elim}). From these plots it becomes evident that the order of magnitude improvement in the reproducibility of *AUC* between subjects that we achieve originates from actively adjusting dosing in response to fluctuations of the rate of elimination. In other words, since tobramycin is excreted unchanged via the kidneys (i.e., it is not metabolized within the body), our PID-controller is finely regulating dosing to match kidney clearance.

this averaged profile, we then defined a time-varying function, which we set as a reference in the PID controller. Employing this to perform the controlled intravenous infusion of tobramycin into a rat we generated a drug profile closely emulating human drug exposure levels, which are characterized by much slower elimination kinetics than those seen in rats (Figure 6). To achieve this, the PID-controller actively

DOI: 10.1021/acsptsci.8b00033
ACS Pharmacol. Transl. Sci. 2018, 1, 110−118

overcomes the rat's rapid excretion of the drug by dosing at a rate that continuously "beats" the drug's elimination half-life.

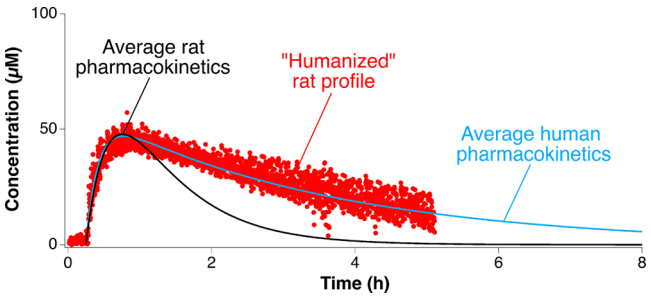

Figure 6. "Humanizing" animal pharmacokinetics. PID-controlled delivery following a programmed pharmacokinetic function that emulates human drug exposure levels creates an unprecedented opportunity to account for interspecies metabolic differences and determine the effects of human-like plasma drug time profiles on human disease being studied in animal models.

The ability to perform metabolism-responsive, feedback-controlled drug delivery based on real-time, in situ concentration measurements has the potential to dramatically improve pharmacological treatment. The decades-long effort to achieve feedback control over blood sugar,[69] for example, has recently delivered an FDA-approved device that is creating unprecedented advances in the treatment of diabetes.[70] Beyond this single, unambiguous success, however, other efforts to achieve feedback-controlled drug delivery remain extremely limited. In one of the few prior examples, blood was continuously drawn from an animal into an ex-vivo microfluidic chip for E-AB analysis before being discarded,[42] and the resultant concentration information was used to perform feedback control of rather limited precision and duration.[71] The only other reports of feedback-controlled drug delivery we are aware of are a set of studies that regulated anesthetic dosing based on input from electrocardiogram- or electromyography-derived measurements of the depth of anesthesia,[72−75] and a study that employed an automated sphygmomanometer to control the dosing of phenylephrine to maintain proper blood pressure.[76] None of these examples, of course, employed real-time, in situ measurements of drugs in the body to inform control because these were simply not available prior to the advent of indwelling E-AB sensors.[28]

E-AB supported feedback control takes advantage of the unmatched properties of the sensing platform to optimally deliver intravenous drugs, but it is also, of course, subject to its limitations and to limitations in drug delivery. Feedback control, for example, can only be performed on drugs that can be delivered continuously via long-term infusion. Likewise it can only be performed on drugs for which E-AB sensors of clinically sufficient specificity are available. This said, the ability to perform negative selections during aptamer development suggests the impact of this may be limited.[77,78] Another potential limitation of E-AB-derived feedback control relates to the duration of the approach, which to date has only been demonstrated to work over periods of 6 h due to anesthetic-exposure limits currently in place per our animal protocols. Efforts to transition such studies to awake animal models to test and extend the duration of the approach are ongoing. Finally, to date we have only explored E-AB sensor placements in the circulatory system; future work will explore the placing of sensors in tissues, opening up the real possibility of feedback control over drug levels at the actual site of therapeutic intervention.

Here we have demonstrated the ability of E-AB-informed feedback control to regulate plasma drug levels in situ in live animals. This unprecedented, high-precision control over plasma drug levels could prove a powerful tool in pharmacological research. The ability to precisely achieve predefined, time-varying drug profiles, for example, would help eliminate the often confounding effects of subject-to-subject pharmacokinetic variability or to emulate the effects of human drug exposure in animal models. And the ability to maintain constant plasma drug concentrations provides a unique opportunity to monitor pharmacokinetic variation with time resolution orders of magnitude better than is possible using traditional (ex vivo) approaches. Finally, by optimizing drug delivery rates many times a minute the resultant fine control over drug plasma concentrations could improve our ability to accurately maintain therapeutic levels even in the face of unexpected changes in health, diet, or drug−drug interactions, and thus represents a significant improvement over state-of-the-art drug delivery. In short, the technology demonstrated here could greatly enhance both the development and delivery of pharmacological treatment.

MATERIALS AND METHODS

Reagents and Materials. Sodium hydroxide, sulfuric acid, tris(hydroxymethyl)aminomethane (Tris), ethylenediaminetetraacetic acid (EDTA), sodium hydrogen phosphate, sodium chloride, potassium chloride, and potassium dihydrogen phosphate were obtained from Fisher Scientific (Waltham, MA). 6-Mercapto-1-hexanol and tris(2-carboxyethyl)-phosphine (TCEP) were obtained from Sigma-Aldrich (St. Louis, MO). Tobramycin sulfate (USP grade) was obtained from Gold BioTechnology, Inc. (St. Louis, MO). All reagents were used as received. A 1X stock solution of phosphate buffered saline (PBS) was prepared containing 10 mM sodium hydrogen phosphate, 2.7 mM potassium chloride, 137 mM sodium chloride, and 1.76 mM potassium phosphate. A 1X stock solution of Tris-EDTA buffer was prepared containing 10 mM Tris-HCl (pH 8.0) and 1 mM EDTA.

Catheters (22 G) and 1 mL syringes were purchased from Becton Dickinson (Franklin Lakes, NJ). PTFE-insulated gold, platinum, and silver wires (75 μm diameter) were purchased from A-M systems. To employ the silver wires as reference electrodes they were immersed in concentrated sodium hypochlorite (commercial bleach) overnight to form a silver chloride film. Heat-shrink polytetrafluoroethylene insulation (PTFE, HS Sub-Lite-Wall, 0.02, 0.005, 0.003 ± 0.001 in, black-opaque, Lot No. 17747112-3), used to electrically insulate gold, silver, and platinum wires, was purchased from ZEUS (Branchburg Township, CA). Custom-made, open ended, mesh-covered three channel connector cables to fabricate in vivo probes were purchased from PlasticsOne (Roanoke, VA).

DNA Aptamer. The tobramycin binding aptamer sequence employed in this work was obtained from previous reports.[28,42] We purchased the methylene-blue-and-thiol-modified DNA from Biosearch Technologies, with sequence

DOI: 10.1021/acsptsci.8b00033
ACS Pharmacol. Transl. Sci. 2018, 1, 110−118

5′−HO−$(CH_2)_6$−S−S−$(CH_2)_6$−OPO_2−O−
GGGACTTGGTTTAGGTAATGAGTCCC−CH_2-
$CHCH_2OH$-$(CH_2)_4$−NH−CO−$(CH_2)_2$−
Methylene Blue-3′

The DNA aptamer was purified through dual HPLC by the supplier and used as received. Upon receipt, each construct was dissolved to 200 μM in 1X Tris-EDTA buffer and frozen at −20 °C in individual aliquots until use.

Electrode Fabrication. The E-AB sensors employed in this work were fabricated as described in previous reports.[32,37] Briefly, segments of pure gold (12 cm in length), platinum (11.5 cm), and silver (11 cm) wire, were cut to make sensors. The insulation at both ends of these wires, about 2 cm, was removed using a surgical blade to allow electrical contact. These were then soldered each to one of the three ends of a connector cable using 60% tin/40% lead rosin-core solder (0.8 mm diameter) and then attached together by applying heat to shrinkable tubing around the body of the wires, except for a small window of about 5 mm at the edge of each wire. The wires were attached in a layered fashion, with the gold wire being insulated alone first, then both gold and platinum wires together, and finally all three wires together. The purpose of this three-layer-thick insulation was to give mechanical strength to the body of the malleable probe. To prevent electrical shorts between wires, different lengths were used for each wire as described above. The sensor window (i.e., the region devoid of insulation) in the gold wire was cut to approximately 3 mm in length. To increase the surface area of the gold working electrodes (to obtain larger peak currents) the sensor surface was roughened electrochemically via immersion in 0.5 M sulfuric acid followed by stepping the potential between $E_{initial}$ = 0.0 V to E_{high} = 2.0 V vs Ag/AgCl, back and forth, for 16 000 pulses.[32] Each potential step was of 20 ms duration with no waiting time in-between pulses. To fabricate sensors an aliquot of the DNA construct was reduced for 30 min at room temperature with a 1000-fold molar excess of tris(2-carboxyethyl)phosphine. A freshly roughened probe was then rinsed in deionized water before being immersed in a solution of the reduced DNA construct at 200 nM in PBS for 1 h at room temperature. Following this the sensor was immersed overnight at 25 °C for 12 h in 5 mM 6-mercapto-1-hexanol in PBS to coat the remaining gold surface. After this, the sensor was rinsed with deionized water and stored in PBS.

Electrochemical Data Acquisition and Processing. The sensors were interrogated via square wave voltammetry by sweeping the electrode potential from 0.0 V to −0.5 V versus Ag/AgCl, using an amplitude of 50 mV, potential step sizes of 1−5 mV, and varying frequencies from 10 to 500 Hz. The files corresponding to each voltammogram were recorded in serial order using macros in CH Instruments software. All square wave measurements were performed using a three-electrode setup as described above and with a CH Instruments Electrochemical workstation (Austin, TX, model 1040C). Postexperiment data processing was carried out in Igor Pro v.7 software. Images were assembled using Adobe Creative Cloud Illustrator using EPS files exported from Igor Pro.

Feedback Control Scripts and Computer Interface. We coded the PID-controller script in MATLAB 2016. Briefly, the program extracts peak currents from square wave voltammograms recorded using different square wave frequencies. Employing this information and a calibration curve collected prior to in vivo measurements (performed in flowing whole blood in vitro),[28] it calculates free-drug concentrations. It then compares these measured concentrations to the reference set point, computes the appropriate dosage to deliver based on the PID-controller response, and correspondingly adjusts the rate with which the pump infuses the drug. We delivered drug doses using the Instrument Control Toolbox module in MATLAB 2016 to communicate with a KD Scientific pump, KDS 200 Legacy Series. The minimum time interval for the actuation of the pump is set by the time it takes to complete the measurement of the voltammograms, which is ∼7 s. In this work we averaged the pump actuation over two points. The magnitude of the gains employed, as well as all other experimental parameters, are included within the full script presented in the Supporting Information Appendix.

In Vitro Testing. Prior to performing in vivo experiments we tested the ability of our PID controller to estimate infusion rates that would maintain constant drug concentrations in vitro in flowing PBS buffer. We did this by connecting a feedback-controlled syringe pump to a 1000 mL beaker modified with a liquid feed inlet and one outlet. We controlled the flow of PBS buffer going into and out of the beaker so that the net volume in the glass vessel remained constant at 300 mL but would be completely replaced with fresh buffer every 20 min (i.e., we simulated rapid drug elimination kinetics in this "glass rat"). We then instructed the controller to hold E-AB-measured drug concentrations constant while challenging with fast buffer washes and tuned the gain magnitudes to maintain the preset concentration within 5% precision (Figure S1). This setting allowed us to tune the value of each of the controller gains to produce drug infusion rates compatible with in vivo experiments.

Animal Procedures. In vivo measurements were performed in male and female Sprague-Dawley rats (4−5 months old) purchased from Charles River Laboratories (Santa Cruz, CA), weighing between 300 and 500 g. All animals were pair-housed in a standard light cycle room (08:00 on, 20:00 off) and allowed ad libitum access to food and water. The experimental protocol was approved by the Institutional Animal Care and Use Committee (IACUC) of the University of California Santa Barbara and adhered to the guidelines given by the NIH Guide for Care and Use of Laboratory Animals (8th edition, National Academy Press, 2011).[79]

For in vivo measurements rats were induced under 5% isoflurane anesthesia in a Plexiglas anesthesia chamber. The rats were then maintained on 2−3% isoflurane gas for the duration of the experiment. While anesthetized, an infusion line was inserted into the left jugular vein of the rats and E-AB sensors were inserted into the opposite, right vein. Briefly, the area above each jugular vein was shaved and cleaned with betadine and 70% ethanol. A small incision was made above each vein, and then each vein was isolated. A small hole was cut into each vein with spring-loaded microscissors. Into one we inserted a silastic catheter constructed with a bent steel cannula with a screw-type connector (Plastics One, Roanoke, VA) and silastic tubing (11 cm, i.d. 0.64 mm, o.d. 1.19 mm, Dow Corning, Midland, MI) for infusions. In the other we inserted the E-AB sensor. Both the E-AB sensor and the infusion line were tied into place with sterile 6−0 silk suture (Fine Science Tools, Foster City, CA), then 30 units of heparin

DOI: 10.1021/acsptsci.8b00033
ACS Pharmacol. Transl. Sci. 2018, 1, 110−118

were infused into the rat prior to the recording of measurements.

All in vivo measurements were performed using a three-electrode setup in which the reference electrode was a silver wire coated with a silver chloride film as described above, and the counter electrode was a platinum wire. A 20 min sensor baseline was established before performing PID-controlled drug infusions. Recordings were taken for up to 6 h, with typical sampling rates of one concentration measurement every 7 s.

■ ASSOCIATED CONTENT

Supporting Information

The Supporting Information is available free of charge on the ACS Publications website at DOI: 10.1021/acsptsci.8b00033.

Setup of our "glass rat" and control experiments (Figures S1); data in support of some of the claims of this manuscript (Figures S2−S6); full copy of our Matlab script (PDF)

■ AUTHOR INFORMATION

Corresponding Authors

*E-mail: kwp@chem.ucsb.edu. Tel.: (805) 893-5558.
*E-mail: netzarroyo@jhmi.edu. Tel.: (410) 955-3569.

ORCID

Netzahualcóyotl Arroyo-Currás: 0000-0002-2740-6276
Gabriel Ortega: 0000-0002-7126-9096
Kevin W. Plaxco: 0000-0003-4772-8771

Author Contributions

N.A.C., T.E.K., and K.W.P. conceived the experiments. N.A.C. and G.O. developed the E-AB sensors and carried out experiments in vitro. N.A.C. and K.L.P. carried out the experiments in vivo. K.L.P. performed all the animal surgeries. T.E.K. created the animal study protocol. N.A.C., G.O., D.C., and J.H. developed the scripts involved in all feedback control experiments. Z.A.P. created the computer interface to run the real-time in vivo measurements. K.L.P. and T.E.K. supervised and enforced approved animal protocols.

Notes

The authors declare no competing financial interest.

■ ACKNOWLEDGMENTS

This work was sponsored in part by the Institute for Collaborative Biotechnologies through Grants W911NF-09-0001 from the U.S. Army Research Office and Grant EB022015 from the National Institutes of Health. G.O. acknowledges financial support through the Postdoctoral Program of the Department of Education of the Basque Government.

■ REFERENCES

(1) Hoover, J. L., Singley, C. M., Elefante, P., DeMarsh, P., Zalacain, M., and Rittenhouse, S. (2017) Reducing antibacterial development risk for gsk1322322 by exploring potential human dose regimens in nonclinical efficacy studies using immunocompetent rats. *Antimicrob. Agents Chemother.*, 959-17.

(2) Thabit, A. K., Monogue, M. L., and Nicolau, D. P. (2016) Eravacycline pharmacokinetics and challenges in defining humanized exposure in vivo. *Antimicrob. Agents Chemother. 60* (8), 5072−5075.

(3) Matsumoto, S., Singley, C. M., Hoover, J., Nakamura, R., Echols, R., Rittenhouse, S., Tsuji, M., and Yamano, Y. (2017) Efficacy of cefiderocol against carbapenem-resistant gram-negative bacilli in immunocompetent-rat respiratory tract infection models recreating human plasma pharmacokinetics. *Antimicrob. Agents Chemother. 61* (9), e00700−17.

(4) Dubé, L., Caillon, J., Gras-Le Guen, C., Jacqueline, C., Kergueris, M.-F., Granry, J.-C., Potel, G., and Bugnon, D. (2003) Simulation of human gentamicin pharmacokinetics in an experimental enterococcus faecalis endocarditis model. *Antimicrob. Agents Chemother. 47* (11), 3663−3666.

(5) LaVan, D. A., McGuire, T., and Langer, R. (2003) Small-scale systems for in vivo drug delivery. *Nat. Biotechnol. 21*, 1184.

(6) Heller, A. (2005) Integrated medical feedback systems for drug delivery. *AIChE J. 51* (4), 1054−1066.

(7) Rosen, H., and Abribat, T. (2005) The rise and rise of drug delivery. *Nat. Rev. Drug Discovery 4*, 381.

(8) Rawson, T. M., O'Hare, D., Herrero, P., Sharma, S., Moore, L. S. P., de Barra, E., Roberts, J. A., Gordon, A. C., Hope, W., Georgiou, P., Cass, A. E. G., and Holmes, A. H. (2018) Delivering precision antimicrobial therapy through closed-loop control systems. *J. Antimicrob. Chemother. 73* (4), 835−843.

(9) Kryscio, D. R., and Peppas, N. A. (2009) Mimicking biological delivery through feedback-controlled drug release systems based on molecular imprinting. *AIChE J. 55* (6), 1311−1324.

(10) Wang, J. (2008) Electrochemical glucose biosensors. *Chem. Rev. 108* (2), 814−825.

(11) Badgaiyan, R. D. (2014) Imaging dopamine neurotransmission in live human brain. *Prog. Brain Res. 211*, 165−182.

(12) Chefer, V. I., Thompson, A. C., Zapata, A., and Shippenberg, T. S. (2009) Overview of brain microdialysis. *Curr. Protoc. Neurosci. 47* (1), 7.1.1−7.1.28.

(13) Gu, H., Varner, E. L., Groskreutz, S. R., Michael, A. C., and Weber, S. G. (2015) In vivo monitoring of dopamine by microdialysis with 1 min temporal resolution using online capillary liquid chromatography with electrochemical detection. *Anal. Chem. 87* (12), 6088−6094.

(14) Parsons, L. H., Koob, G. F., and Weiss, F. (1995) Extracellular serotonin is decreased in the nucleus accumbens during withdrawal from cocaine self-administration. *Behav. Brain Res. 73* (1−2), 225−228.

(15) Wang, M., Roman, G. T., Schultz, K., Jennings, C., and Kennedy, R. T. (2008) Improved temporal resolution for in vivo microdialysis by using segmented flow. *Anal. Chem. 80* (14), 5607−5615.

(16) Bucher, E. S., and Wightman, R. M. (2015) Electrochemical analysis of neurotransmitters. *Annu. Rev. Anal. Chem. 8*, 239−261.

(17) Naylor, E., Aillon, D. V., Gabbert, S., Harmon, H., Johnson, D. A., Wilson, G. S., and Petillo, P. A. (2011) Simultaneous real-time measurement of eeg/emg and l-glutamate in mice: A biosensor study of neuronal activity during sleep. *J. Electroanal. Chem. 656* (1), 106−113.

(18) Wilson, G. S., and Gifford, R. (2005) Biosensors for real-time in vivo measurements. *Biosens. Bioelectron. 20* (12), 2388−2403.

(19) Shon, Y.-M., Chang, S.-Y., Tye, S. J., Kimble, C. J., Bennet, K. E., Blaha, C. D., and Lee, K. H. (2010) Comonitoring of adenosine and dopamine using the wireless instantaneous neurotransmitter concentration system: Proof of principle. *J. Neurosurg. 112* (3), 539−548.

(20) Wilson, G. S., and Hu, Y. (2000) Enzyme-based biosensors for in vivo measurements. *Chem. Rev. 100* (7), 2693−2704.

(21) Damsma, G., Westerink, B. H. C., de Vries, J. B., Van den Berg, C. J., and Horn, A. S. (1987) Measurement of acetylcholine release in freely moving rats by means of automated intracerebral dialysis. *J. Neurochem. 48* (5), 1523−1528.

(22) Feldman, B., Brazg, R., Schwartz, S., and Weinstein, R. (2003) A continuous glucose sensor based on wired enzyme technology - results from a 3-day trial in patients with type 1 diabetes. *Diabetes Technol. Ther. 5* (5), 769−779.

(23) Mastrototaro, J., Shin, J., Marcus, A., and Sulur, G. (2008) The accuracy and efficacy of real-time continuous glucose monitoring

DOI: 10.1021/acsptsci.8b00033
ACS Pharmacol. Transl. Sci. 2018, 1, 110−118

sensor in patients with type 1 diabetes. *Diabetes Technol. Ther. 10* (5), 385−390.
(24) Mastrototaro, J. J. (2000) The minimed continuous glucose monitoring system. *Diabetes Technol. Ther. 2* (supplement1), 13−18.
(25) Mehrotra, P. (2016) Biosensors and their applications − a review. *J. Oral Biol. Craniofac. Res. 6* (2), 153−159.
(26) Meyerhoff, C., Bischof, F., Mennel, F. J., Sternberg, F., Bican, J., and Pfeiffer, E. F. (1993) On line continuous monitoring of blood lactate in men by a wearable device based upon an enzymatic amperometric lactate sensor. *Biosens. Bioelectron. 8* (9), 409−414.
(27) Clark, L. C., and Lyons, C. (1962) Electrode systems for continuous monitoring in cardiovascular surgery. *Ann. N. Y. Acad. Sci. 102* (1), 29−45.
(28) Arroyo-Currás, N., Somerson, J., Vieira, P. A., Ploense, K. L., Kippin, T. E., and Plaxco, K. W. (2017) Real-time measurement of small molecules directly in awake, ambulatory animals. *Proc. Natl. Acad. Sci. U. S. A. 114* (4), 645−650.
(29) Schoukroun-Barnes, L. R., Macazo, F. C., Gutierrez, B., Lottermoser, J., Liu, J., and White, R. J. (2016) Reagentless, structure-switching, electrochemical aptamer-based sensors. *Annu. Rev. Anal. Chem. 9* (1), 163−181.
(30) Vallée-Bélisle, A., and Plaxco, K. W. (2010) Structure-switching biosensors: Inspired by nature. *Curr. Opin. Struct. Biol. 20* (4), 518−526.
(31) Lubin, A. A., and Plaxco, K. W. (2010) Folding-based electrochemical biosensors: The case for responsive nucleic acid architectures. *Acc. Chem. Res. 43* (4), 496−505.
(32) Arroyo-Currás, N., Scida, K., Ploense, K. L., Kippin, T. E., and Plaxco, K. W. (2017) High surface area electrodes generated via electrochemical roughening improve the signaling of electrochemical aptamer-based biosensors. *Anal. Chem. 89* (22), 12185−12191.
(33) White, R. J., Phares, N., Lubin, A. A., Xiao, Y., and Plaxco, K. W. (2008) Optimization of electrochemical aptamer-based sensors via optimization of probe packing density and surface chemistry. *Langmuir 24* (18), 10513−10518.
(34) Xiao, Y., Lubin, A. A., Heeger, A. J., and Plaxco, K. W. (2005) Label-free electronic detection of thrombin in blood serum by using an aptamer-based sensor. *Angew. Chem., Int. Ed. 44* (34), 5456−5459.
(35) White, R. J., and Plaxco, K. W. (2010) Exploiting binding-induced changes in probe flexibility for the optimization of electrochemical biosensors. *Anal. Chem. 82* (1), 73−76.
(36) Dauphin-Ducharme, P., and Plaxco, K. W. (2016) Maximizing the signal gain of electrochemical-DNA sensors. *Anal. Chem. 88* (23), 11654−11662.
(37) Arroyo-Currás, N., Dauphin-Ducharme, P., Ortega, G., Ploense, K. L., Kippin, T. E., and Plaxco, K. W. (2018) Subsecond-resolved molecular measurements in the living body using chronoamperometrically interrogated aptamer-based sensors. *ACS Sensors 3* (2), 360−366.
(38) Ferapontova, E. E., Olsen, E. M., and Gothelf, K. V. (2008) An rna aptamer-based electrochemical biosensor for detection of theophylline in serum. *J. Am. Chem. Soc. 130* (13), 4256−4258.
(39) Liu, Y., Tuleouva, N., Ramanculov, E., and Revzin, A. (2010) Aptamer-based electrochemical biosensor for interferon gamma detection. *Anal. Chem. 82* (19), 8131−8136.
(40) Rowe, A. A., Miller, E. A., and Plaxco, K. W. (2010) Reagentless measurement of aminoglycoside antibiotics in blood serum via an electrochemical, ribonucleic acid aptamer-based biosensor. *Anal. Chem. 82* (17), 7090−7095.
(41) Wu, J., Chu, H., Mei, Z., Deng, Y., Xue, F., Zheng, L., and Chen, W. (2012) Ultrasensitive one-step rapid detection of ochratoxin a by the folding-based electrochemical aptasensor. *Anal. Chim. Acta 753*, 27−31.
(42) Ferguson, B. S., Hoggarth, D. A., Maliniak, D., Ploense, K., White, R. J., Woodward, N., Hsieh, K., Bonham, A. J., Eisenstein, M., Kippin, T. E., Plaxco, K. W., and Soh, H. T. (2013) Real-time, aptamer-based tracking of circulating therapeutic agents in living animals. *Sci. Transl. Med. 5* (213), 213ra165.
(43) Yu, Z.-g., and Lai, R. Y. (2018) A reagentless and reusable electrochemical aptamer-based sensor for rapid detection of ampicillin in complex samples. *Talanta 176*, 619−624.
(44) Pang, J., Zhang, Z., and Jin, H. (2016) Effect of structure variation of the aptamer-DNA duplex probe on the performance of displacement-based electrochemical aptamer sensors. *Biosens. Bioelectron. 77*, 174−181.
(45) Santos-Cancel, M., and White, R. J. (2017) Collagen membranes with ribonuclease inhibitors for long-term stability of electrochemical aptamer-based sensors employing rna. *Anal. Chem. 89* (10), 5598−5604.
(46) Fetter, L., Richards, J., Daniel, J., Roon, L., Rowland, T. J., and Bonham, A. J. (2015) Electrochemical aptamer scaffold biosensors for detection of botulism and ricin toxins. *Chem. Commun. 51* (82), 15137−15140.
(47) Yu, P., Liu, Y., Zhang, X., Zhou, J., Xiong, E., Li, X., and Chen, J. (2016) A novel electrochemical aptasensor for bisphenol a assay based on triple-signaling strategy. *Biosens. Bioelectron. 79*, 22−28.
(48) Somerson, J., and Plaxco, K. (2018) Electrochemical aptamer-based sensors for rapid point-of-use monitoring of the mycotoxin ochratoxin a directly in a food stream. *Molecules 23* (4), 912.
(49) Li, H., Dauphin-Ducharme, P., Arroyo-Currás, N., Tran, C. H., Vieira, P. A., Li, S., Shin, C., Somerson, J., Kippin, T. E., and Plaxco, K. W. (2017) A biomimetic phosphatidylcholine-terminated monolayer greatly improves the in vivo performance of electrochemical aptamer-based sensors. *Angew. Chem., Int. Ed. 56* (26), 7492−7495.
(50) Begg, E. J., Barclay, M. L., and Kirkpatrick, C. J. M. (1999) The therapeutic monitoring of antimicrobial agents. *Br. J. Clin. Pharmacol. 47* (1), 23−30.
(51) Coulthard, K. P., Peckham, D. G., Conway, S. P., Smith, C. A., Bell, J., and Turnidge, J. (2007) Therapeutic drug monitoring of once daily tobramycin in cystic fibrosis—caution with trough concentrations. *J. Cystic Fibrosis 6* (2), 125−130.
(52) Sánchez-Alcaraz, A., Vargas, A., Quintana, M. B., Rocher, A., Querol, J. M., Poveda, J. L., and Hermenegildo, M. (1998) Therapeutic drug monitoring of tobramycin: Once-daily versus twice-daily dosage schedules. *J. Clin. Pharm. Ther. 23* (5), 367−373.
(53) Kiam Heong, A., Chong, G., and Yun, L. (2005) Pid control system analysis, design, and technology. *IEEE T. CONTR. SYST. T. 13* (4), 559−576.
(54) Åström, K. J., and Hägglund, T. (1995) *Pid controllers: Theory, Design, and Tuning*, Vol. 2, Isa Research Triangle Park, , NC.
(55) Lee, C., Walker, S. A. N., Walker, S. E., Seto, W., Simor, A., and Jeschke, M. (2017) A prospective study evaluating tobramycin pharmacokinetics and optimal once daily dosing in burn patients. *Burns 43* (8), 1766−1774.
(56) Berry, V., Hoover, J., Singley, C., and Woodnutt, G. (2005) Comparative bacteriological efficacy of pharmacokinetically enhanced amoxicillin-clavulanate against streptococcus pneumoniae with elevated amoxicillin mics and Haemophilus influenzae. *Antimicrob. Agents Chemother. 49* (3), 908−915.
(57) Seifert, H., Körber-Irrgang, B., Kresken, M., Gobel, U., Swidsinski, S., Rath, P.-M., Steinmann, J., MacKenzie, C, Mutters, R., Schubert, S., et al. (2017) In-vitro activity of ceftolozane/tazobactam against pseudomonas aeruginosa and enterobacteriaceae isolates recovered from hospitalized patients in germany. *Int. J. Antimicrob. Agents 51* (2), 227−234.
(58) Loftsson, T. (2015) Chapter 2: basic concepts of pharmacokinetics. In *Essential Pharmacokinetics*, pp 9−84, Academic Press, Boston.
(59) Longson, D., Mills, J. N., Thomas, S., and Yates, P. A. (1956) Handling of phosphate by the human kidney at high plasma concentrations. *J. Physiol. 131* (2), 555−571.
(60) Prasad, N., and Bhadauria, D. (2013) Renal phosphate handling: Physiology. *Indian J. Endocrinol. Metab. 17* (4), 620−627.
(61) Abdul-Aziz, M. H., Dulhunty, J. M., Bellomo, R., Lipman, J., and Roberts, J. A. (2012) Continuous beta-lactam infusion in critically ill patients: The clinical evidence. *Ann. Intensive Care 2* (1), 37.

DOI: 10.1021/acsptsci.8b00033
ACS Pharmacol. Transl. Sci. 2018, 1, 110−118

(62) Craig, W. A., and Ebert, S. C. (1992) Continuous infusion of beta-lactam antibiotics. *Antimicrob. Agents Chemother. 36*, 2577.
(63) Dulhunty, J. M., Roberts, J. A., Davis, J. S., Webb, S. A. R., Bellomo, R., Gomersall, C., Shirwadkar, C., Eastwood, G. M., Myburgh, J., Paterson, D. L., Starr, T., Paul, S. K., and Lipman, J. (2015) A multicenter randomized trial of continuous versus intermittent β-lactam infusion in severe sepsis. *Am. J. Respir. Crit. Care Med. 192* (11), 1298−1305.
(64) Mohd Hafiz, A. A., Staatz, C. E., Kirkpatrick, C. M., Lipman, J., and Roberts, J. A. (2012) Continuous infusion vs. Bolus dosing: Implications for beta-lactam antibiotics. *Minerva Anestesiol 78* (1), 94−104.
(65) Mouton, J. W., and Vinks, A. A. (2007) Continuous infusion of beta-lactams. *Curr. Opin. Crit. Care 13* (5), 598−606.
(66) Wilkinson, G. R. (2005) Drug metabolism and variability among patients in drug response. *N. Engl. J. Med. 352* (21), 2211−2221.
(67) Levy, J., Smith, A. L., Koup, J. R., Williams-Warren, J., and Ramsey, B. (1984) Disposition of tobramycin in patients with cystic fibrosis: A prospective controlled study. *J. Pediatr. 105* (1), 117−124.
(68) Ratjen, F., Brockhaus, F., and Angyalosi, G. (2009) Aminoglycoside therapy against pseudomonas aeruginosa in cystic fibrosis: A review. *J. Cystic Fibrosis 8* (6), 361−369.
(69) Hovorka, R. (2011) Closed-loop insulin delivery: From bench to clinical practice. *Nat. Rev. Endocrinol. 7*, 385.
(70) Food and Drug Administration Fda authorizes first fully interoperable continuous glucose monitoring system, streamlines review pathway for similar devices. https://www.fda.gov/NewsEvents/Newsroom/PressAnnouncements/ucm602870.htm (accessed 03/27/2018).
(71) Mage, P. L., Ferguson, B. S., Maliniak, D., Ploense, K. L., Kippin, T. E., and Soh, H. T. (2017) Closed-loop control of circulating drug levels in live animals. *Nat. Biomed. Eng. 1*, 0070.
(72) Schwilden, H., and Stoeckel, H. (1993) Closed-loop feedback controlled administration of alfentanil during alfentanil-nitrous oxide anaesthesia. *Br. J. Anaesth. 70* (4), 389−393.
(73) Schwilden, H., Stoeckel, H., and SchÜTtler, J. (1989) Closed-loop feedback control of propofol anaesthesia by quantitative eeg analysis in humans. *Br. J. Anaesth. 62* (3), 290−296.
(74) Mendonça, T., and Lago, P. (1998) Pid control strategies for the automatic control of neuromuscular blockade. *Control Eng. Pract. 6* (10), 1225−1231.
(75) Liu, N., Chazot, T., Hamada, S., Landais, A., Boichut, N., Dussaussoy, C., Trillat, B., Beydon, L., Samain, E., Sessler, D. I., and Fischler, M. (2011) Closed-loop coadministration of propofol and remifentanil guided by bispectral index: A randomized multicenter study. *Anesth. Analg. 112* (3), 546−557.
(76) Ngan Kee, W. D., Khaw, K. S., and Ng, F. F. (2004) Comparison of phenylephrine infusion regimens for maintaining maternal blood pressure during spinal anaesthesia for caesarean section. *Br. J. Anaesth. 92* (4), 469−474.
(77) Yang, K.-A., Barbu, M., Halim, M., Pallavi, P., Kim, B., Kolpashchikov, D., Pecic, S., Taylor, S., Worgall, T. S., and Stojanovic, M. N. (2014) Recognition and sensing of low-epitope targets via ternary complexes with oligonucleotides and synthetic receptors. *Nat. Chem. 6* (11), 1003−1008.
(78) Nakatsuka, N., Yang, K.-A., Abendroth, J. M., Cheung, K., Xu, X., Yang, H., Zhao, C., Zhu, B., Rim, Y. S., Yang, Y., Weiss, P. S., Stojanović, M. N., and Andrews, A. M. (2018) Aptamer−field-effect transistors overcome debye length limitations for small-molecule sensing. *Science*, eaao6750.
(79) Committee for the Update of the Guide for the Care and Use of Laboratory Animals. (2011) *Guide for the care and use of laboratory animals*, 8th ed., The National Academies Press.

DOI: 10.1021/acsptsci.8b00033
ACS Pharmacol. Transl. Sci. 2018, 1, 110−118